Aalborg Universitet

A Study on EMF Exposure Assessments With Different Metrics for User Equipment Antennas at 6 and 10 GHz

Zhekov, Stanislav Stefanov; Yao, Ming; Di Paola, Carla; Xu, Bo; Zhang, Shuai

A Study on EMF Exposure Assessments With Different Metrics for User Equipment Antennas at 6 and 10 GHz

Stanislav Stefanov Zhekov, Ming Yao, Carla Di Paola, Bo Xu, and Shuai Zhang

Abstract—User equipment (UE) needs to comply with regulations limiting the exposure of the human body to electromagnetic fields (EMFs). In this paper, three exposure metrics including specific absorption rate (SAR), incident power density (IPD), and absorbed power density (APD) are quantified for different UE antenna designs. The exposure ratios of the metrics are quantified according to the relevant EMF limit values. The investigations are performed at or close to the transition frequency between different exposure metrics - the range 6-10 GHz being of research interest and currently attracting attention for emerging mobile technologies. The study demonstrates that the IPD does not correlate well with the APD, within the investigated frequency region, when the reactive near-field of the antenna is of interest. This is in accordance with the ICNIRP 2020 guidelines meaning that the absorbed power density should be used for compliance purposes. For validation purposes, prototypes are fabricated, and SAR and incident power density are measured. The average difference between the numerical and experimental results is 0.4 dB for SAR and 0.9 dB for the incident power density, meaning that good agreement between simulations and measurements is obtained.

Index Terms—absorbed power density, antenna, electromagnetic field exposure, incident power density, specific absorption rate, user equipment.

I. Introduction

USER equipment (UE) has become an integral part of people's everyday life. The constant desire for better quality-of-service has been the driving force behind the development from the first (1G) to the fifth generation (5G) mobile communication systems. The 5G spectra are divided into two frequency ranges (FRs) including FR1 (sub-7 GHz) [1] and FR2 (from 24.25 to 71.0 GHz) [2]. Discussions regarding the sixth generation (6G) mobile communication systems have already started [3]. The spectrum around 10 GHz is seen as potential bands for future cellular networks, as the industry and the International Telecommunication Union (ITU) have begun to look into possibilities to use them [4].

There are two aspects to be considered when studying the interaction between antennas and the human body - the antenna performance and the human exposure. On one side, the vicinity of the lossy human tissue to the UE deteriorates its antenna operation. For example, the antenna input impedance changes and therefore the matching and operating bandwidth. A fraction of the radiated power is absorbed in the human tissue leading to reduction in the antenna radiation efficiency. Furthermore, the radiation pattern is distorted due to the human body blockage. There are multiple studies in the literature on the influence of the human body on the UE antenna performance, and some of them can be found in [5]–[12]. All mentioned effects of the human body on the antenna have negative impact on the performance of the mobile communication system [13]–[16].

The other aspect of the interaction between the UE antenna and the human body is related to the electromagnetic field (EMF) exposure. EMF exposure limits are set in international guidelines, e.g., [17], [18], and by national authorities, e.g., [19]. Compliance of UE with the set limits [20]–[23] is demonstrated by means of methods and procedures specified by standards, e.g., [24].

The International Commission on Non-Ionizing Radiation Protection (ICNIRP) and the IEEE have published guidelines defining basic restrictions (ICNIRP) or dosimetric reference limits (IEEE), [17], [18]. Below 6 GHz, the 6-minute averaged basic restrictions (dosimetric reference limits) applicable for local exposure are specified in terms of specific absorption rate (SAR). SAR is to be averaged over a volume of tissue in the shape of a cube with a mass of 10 g. Evaluating EMF compliance of UE with SAR is a well-established practice. Above 6 GHz, the corresponding basic restrictions are expressed in terms of absorbed power density (APD). The APD should be averaged over a square surface of 4 cm^2. Above 30 GHz, twice the limit value with an averaging square area of 1 cm^2 should not be exceeded either [17]. The basic restrictions refer to quantities inside an exposed body which can be difficult to evaluate. Therefore, reference levels (ICNIRP) or exposure reference levels (IEEE) are derived from the basic restrictions under worst-case conditions, to demonstrate compliance using free-space quantities that are more easily evaluated. Above 6 GHz, the reference levels are specified in terms of incident power density (IPD) which is intended to be averaged in the same manner as the APD; however since the IPD, above 6 GHz, does not appropriately correlate with the APD in the reactive near-field region, the reference levels cannot be used to determine compliance in the reactive near-field, and so basic restrictions must be assessed [17]. The APD and IPD assessments for UE antennas above 6 GHz have been conducted, e.g., in [25]–[30] but a comparative analysis between the two metrics when used to assess compliance of portable devices is not available. A way to evaluate APD between 6 and 10 GHz based on measurements of SAR has been proposed in [31] and it is part of the IEC Publicly Available Specification (PAS) 63446 [32]. The same methodology is investigated here for the considered
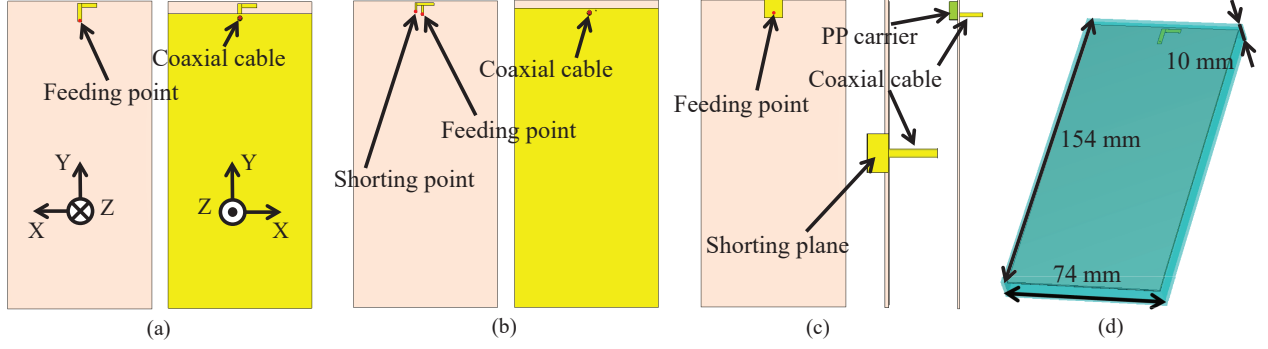
Fig. 1: Studied antennas: (a) planar dipole, front view and back view; (b) IFA, front view and back view; and (c) PIFA, front view, top view, and side view. The antenna placed inside the mobile phone case (semi-transparent for better visualization) is presented in (d). With yellow color is presented metal, while the other colors mark different dielectric materials.

UE antennas.

In the US, below 6 GHz, the Federal Communications Commission (FCC) sets different SAR limit values and averaging mass from those of ICNIRP and IEEE. The averaging is over a cubic volume of tissue with mass of 1 g. Above 6 GHz, the FCC limits are defined in terms of IPD to be averaged over a 4 cm^2 square area [33]. In the frequency range between 6-7 GHz, for the highest SAR test configurations also the IPD is to be measured for portable devices operating according to interim requirement [34].

This paper aims to verify ICNIRP requirement [17] demanding APD, rather than IPD, to be used in the reactive near-field of a source by comparing the exposure ratio obtained using these two metrics for realistic UE antenna designs and for operating frequencies between 6 and 10 GHz. Then, a similar comparison is done with respect to IPD and SAR averaged over 1-g, as both metrics need to be considered between 6 and 7 GHz when testing EMF compliance according to the FCC interim requirements [34]. At last, the APD approximation formulae proposed recently in [31] are examined with the used antennas.

The paper is organized as follows. In Section II the designs of the antennas, phantom, and exposure metrics used for the investigation are introduced. The numerical results for the exposure levels and exposure ratios are presented in Section III. Measurement results for the different metrics are presented in Section V. Finally, the conclusion is given in Section VI.

II. Study Scenarios

A. Antennas

Three types of antennas were used in the study - planar dipole (labeled as "dipole" in the rest of the paper), inverted-F antenna (IFA), and planar inverted-F antenna (PIFA). These antennas were selected because they are representative for radiators used in UE, e.g., [5], [8], [9], [15], [35]–[38]. The geometry of each radiator is shown in Fig. 1(a)-(c). The metal used for making the antennas and the ground plane (and the shorting plane for the PIFA antenna) was copper with electrical conductivity of $\sigma = 5.8 \times 10^7$ S/m and thickness of 0.035 mm. The antenna and the ground plane were printed on
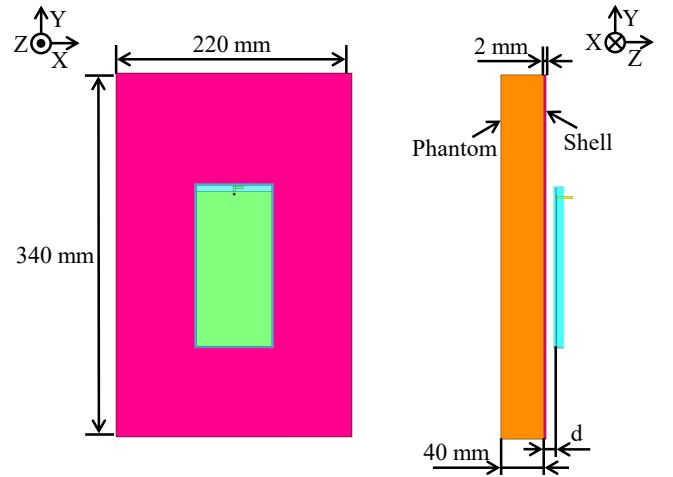

Fig. 2: Phantom and shell used in the study. The top view and the side view are given.

the opposite sides of a FR4 substrate with size of 150 mm $\times$ 70 mm $\times$ 0.8 mm, relative permittivity $\epsilon_r = 4.3$, and loss tangent $\tan(\delta) = 0.025$. The PIFA antenna was placed on a carrier made of polypropylene (PP) plastic with $\epsilon_r = 2.2$ and $\tan(\delta) = 0.0015$ [39]. The antennas were fed by using a standard coaxial cable. Each printed circuit board (PCB) was enclosed by a hollow plastic housing, made from acrylonitrile butadiene styrene (ABS) plastic with $\epsilon_r = 2.55$, $\tan(\delta) = 0.005$. The size of the plastic housing was 154 mm$\times$74 mm$\times$ 10 mm, as shown in Fig. 1(d), and the thickness was 1 mm. The distance between the top surface of the antenna to the corresponding inner wall of the plastic housing was 1 mm. This plastic housing mimicked a mobile phone case. For each antenna type, two radiators were developed - one operating at 6 and one at 10 GHz, as these are the lower and upper bound of the frequency range of interest.

B. Phantom

A homogeneous phantom was used in the study. The phantom had $\epsilon_r = 35.10$ and $\sigma = 5.48$ S/m at 6 GHz, and $\epsilon_r = 30.40$ and $\sigma = 10.40$ S/m at 10 GHz, as specified in [24]. The size of the phantom was 220 mm $\times$ 360 mm $\times$ 40 mm.

A layer of lossless material with $\epsilon_r = 3.7$ [31] and size $220\,\text{mm} \times 360\,\text{mm} \times 2\,\text{mm}$ was used to mimic the phantom shell (labeled as "shell" in the rest of the paper) as specified in [24]. Fig. 2 shows the phantom with the shell and the antenna. d is the distance between the antenna surface and the phantom surface along z-axis (the distance between the mobile phone case and the phantom shell is 4 mm smaller than d). In order to suppress undesired back reflection, the side and back walls of the phantom and the side walls of the shell were touching the perfectly matched layer (PML) boundaries in the computational domain. Thus, infinitely large phantom and shell were mimicked.

C. Exposure Metrics

Three exposure metrics were considered:

- SAR (W/kg) is defined as [17]:

$$SAR = \frac{\sigma|\vec{E}|^2}{2\rho} \qquad (1)$$

where ρ is the mass density (kg/m^3) of the tissue. $|\vec{E}|$ is the magnitude of the electric field in the human tissue (V/m). Two spatial averaging schemes for SAR are adopted: 1) in [17], [18], SAR is averaged over a volume containing a mass of 10 g of tissue, and the peak 10-g averaged value, SAR_{10g}, should not exceed the limit $SAR_{10g,\text{limit}} = 2$ W/kg applicable below 6 GHz; and 2) for the FCC requirements, SAR is averaged over 1 g of tissue, and the peak 1-g averaged SAR, SAR_{1g}, should not exceed the limit $SAR_{1g,\text{limit}} = 1.6$ W/kg [19].

- APD - S_{ab} (W/m^2) is defined as [17]:

$$S_{\text{ab}} = \frac{1}{A} \iint_A dx\,dy \int_0^{z_{\max}} \rho(x,y,z)SAR(x,y,z)\,dz \qquad (2)$$

where the body surface is at $z = 0$, and $z_{\max}$ is the depth of the body at the corresponding region, and A is the averaging area (m^2). A square surface with size $2\,\text{cm} \times 2\,\text{cm}$ (4 cm^2) was used for spatial averaging for APD. The averaging space was oriented such that the xy-plane was parallel to the phantom surface (same as the coordinate system shown in Fig. 2). The limit value for the APD is $S_{\text{ab,limit}} = 20$ W/m^2, applicable above 6 GHz, according to ICNIRP [17].

- IPD - S_{inc} (W/m^2) - the original definition of IPD is the amount of power flow through a unit area, i.e., only the normal component of the Poynting vector across the surface is used [40]:

$$S_{\text{inc},1} = \frac{1}{2A} \iint_A \text{Re}(\vec{E} \times \vec{H}^*) \cdot \vec{u}_z\,dx\,dy \qquad (3.1)$$

where $\vec{E}$ and $\vec{H}$ are the complex electric and magnetic field on the surface of interest, respectively; (*) indicates complex conjugate, $\vec{u}_z$ is the unit vector normal to the surface, and A is the averaging area (m^2) - the same as for APD. In [40], all three components (magnitude of the real part) of the Poynting vector are considered in the IPD calculation:
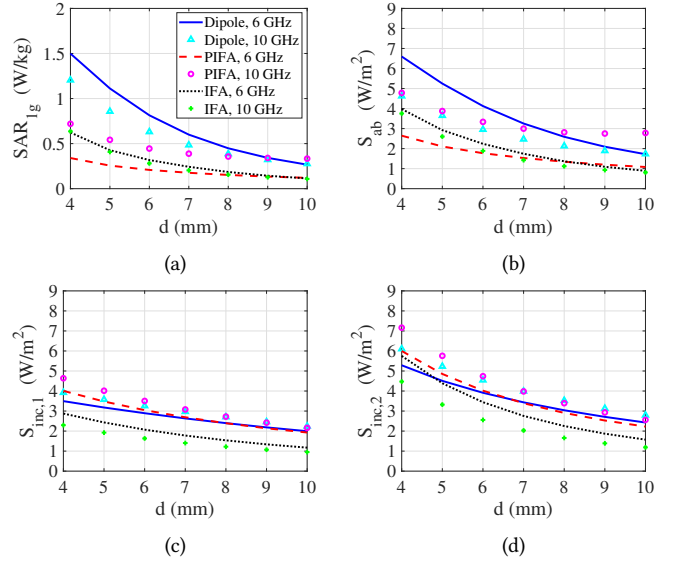

Fig. 3: Simulated peak value for: (a) SAR_{1g}, (b) S_{ab}, (c) $S_{\text{inc},1}$, and (d) $S_{\text{inc},2}$ at 6 and 10 GHz for different evaluation distance d.

$$S_{\text{inc},2} = \frac{1}{2A} \iint_A ||\text{Re}(\vec{E} \times \vec{H}^*)||\,dx\,dy \qquad (3.3)$$

For the ICNIRP guidelines, the IPD limits above 6 GHz is given by $S_{\text{inc,limit}} = 55/f_G^{0.177}$, where f_G is the frequency of interest in GHz [17]. Then, $S_{\text{inc,limit}} = 40.1$ W/m^2 at 6 GHz and $S_{\text{inc,limit}} = 36.6$ W/m^2 at 10 GHz. The FCC limit value above 6 GHz is $S_{\text{inc,limit}} = 10$ W/m^2, regardless of the frequency [19].

III. Simulation Results

All numerical studies were performed by using CST Studio Suite 2021. The size of the mesh cells used for the phantom and the shell was smaller than 0.25 mm at both 6 and 10 GHz. This cell size should ensure good sampling of the fields. The IPD is evaluated in free space, so for its evaluation, the dielectric properties of the flat phantom were replaced by those for vacuum but the same mesh cell sizes were kept. Thus, it was ensured that no difference in the results for the exposure metrics raises due to the change in the meshing.

All exposure metrics were normalized with regard to accepted power of 7 dBm. Normalization to the accepted power was used to ensure that all antennas are matched regardless of whether they operate in free space or close to the phantom. It can be mentioned that the difference in the simulated radiation efficiency between the different antennas is less than 0.5 dB. Thus, this metric is not so critical if the results for different antennas are compared with each other.

A. Exposure Levels

To get an insight about the behavior of the exposure, simulations for multiple distances between the antenna and the phantom were conducted. The selected distances d (see Fig. 2) were from 4 mm (the mobile phone case touches the shell of the phantom) to 10 mm (this corresponds to

6 mm distance between the phone case and phantom shell) with a 1-mm step. Such distances are normally selected for EMF compliance testing of small wireless devices [41]. For the three studied antennas, the peak values of all exposure metrics at the two frequencies and for all investigated d are given in Fig. 3. These results show that: 1) the peak values of different exposure metrics decrease with increasing d; and 2) whether the exposure is larger at 6 or at 10 GHz depends on the antenna design, frequency. However, it should be kept in mind that the study is limited in terms of antennas, frequencies, and distances.

B. Exposure Ratios

To compare different exposure metrics, the quantity *exposure ratio* is defined as the ratio between the peak value for a certain exposure metric and the corresponding limit value for that metric:

$$ER_{\mathrm{SAR1g}} = SAR_{1\mathrm{g}}/SAR_{1\mathrm{g,limit}} \tag{4.1}$$

$$ER_{S_{\mathrm{ab}}} = S_{\mathrm{ab}}/S_{\mathrm{ab,limit}} \tag{4.2}$$

$$ER_{S_{\mathrm{inc,1}}} = S_{\mathrm{inc,1}}/S_{\mathrm{inc,1,limit}} \tag{4.3}$$

$$ER_{S_{\mathrm{inc,2}}} = S_{\mathrm{inc,2}}/S_{\mathrm{inc,2,limit}} \tag{4.4}$$

TABLE I: Peak exposure ratios (ER) for S_{ab}, $S_{\mathrm{inc,1}}$, and $S_{\mathrm{inc,2}}$, when the ICNIRP and IEEE guidelines are considered, at 6 GHz for different distances d obtained by simulations.

Antenna	d (mm)	Exposure ratio		
		$ER_{S_{\mathrm{ab}}}$	$ER_{S_{\mathrm{inc,1}}}$	$ER_{S_{\mathrm{inc,2}}}$
Dipole	4	0.33	0.09	0.13
	5	0.26	0.08	0.11
	6	0.21	0.07	0.10
	7	0.16	0.07	0.09
	8	0.13	0.06	0.08
	9	0.10	0.05	0.07
	10	0.09	0.05	0.06
PIFA	4	0.13	0.10	0.15
	5	0.11	0.09	0.12
	6	0.09	0.08	0.10
	7	0.08	0.07	0.08
	8	0.07	0.06	0.07
	9	0.06	0.05	0.06
	10	0.05	0.05	0.06
IFA	4	0.20	0.07	0.14
	5	0.15	0.06	0.11
	6	0.11	0.05	0.09
	7	0.09	0.04	0.07
	8	0.07	0.04	0.06
	9	0.05	0.03	0.05
	10	0.05	0.03	0.04

The results for the exposure ratio of each metric for the three antennas are sorted in two groups:

1) ICNIRP and IEEE guidelines: The first group includes S_{ab}, and the two definitions of the IPD - $S_{\mathrm{inc,1}}$ and $S_{\mathrm{inc,2}}$ with regard to the respective ICNIRP limit values. The exposure ratio results of this group are presented in Tables I and II at 6 and 10 GHz, respectively.

When all studied cases are considered together, the following can be observed from the data:

- The exposure ratios of $S_{\mathrm{inc,1}}$ (IPD when the normal component of the Poynting vector across the surface

TABLE II: Peak exposure ratios (ER) for S_{ab}, $S_{\mathrm{inc,1}}$, $S_{\mathrm{inc,2}}$, when the ICNIRP and IEEE guidelines are considered, at 10 GHz for different distances d obtained by simulations.

Antenna	d (mm)	Exposure ratio		
		$ER_{S_{\mathrm{ab}}}$	$ER_{S_{\mathrm{inc,1}}}$	$ER_{S_{\mathrm{inc,2}}}$
Dipole	4	0.23	0.11	0.17
	5	0.18	0.10	0.14
	6	0.15	0.09	0.12
	7	0.12	0.08	0.11
	8	0.11	0.07	0.10
	9	0.09	0.07	0.09
	10	0.09	0.06	0.08
PIFA	4	0.24	0.13	0.20
	5	0.19	0.11	0.16
	6	0.17	0.10	0.13
	7	0.15	0.08	0.11
	8	0.14	0.07	0.09
	9	0.14	0.07	0.08
	10	0.14	0.06	0.07
IFA	4	0.19	0.06	0.12
	5	0.13	0.05	0.09
	6	0.09	0.04	0.07
	7	0.07	0.04	0.06
	8	0.06	0.03	0.05
	9	0.05	0.03	0.04
	10	0.04	0.03	0.03

is considered) are lower than those of S_{ab} with the mean difference of 2.6 dB at both studied frequencies. The range within which $ER_{S_{\mathrm{ab}}}$ is higher than $ER_{S_{\mathrm{inc,1}}}$ is from 0.5 to 5.8 dB.

- The exposure ratios of $S_{\mathrm{inc,2}}$ (IPD when the magnitude of the real part of the Poynting vector is used) is on average 1.1 dB and 1.2 dB lower than those of S_{ab} at 6 and 10 GHz. Taking all study cases together, it is found that the exposure ratios of S_{ab} are between 0.6 dB lower and 4.0 dB higher than those of $S_{\mathrm{inc,2}}$. Only for PIFA antenna at 6 GHz, $ER_{S_{\mathrm{inc,2}}}$ is observed to be larger (within the range from 0.1 to 0.6 dB) than $ER_{S_{\mathrm{ab}}}$. In total, S_{ab} has higher exposure ratio in 14 out of 21 cases (3 antennas x 7 distances) at 6 GHz and in all 21 cases at 10 GHz.

It is to be emphasized that according to ICNIRP, the IPD limits are not applicable in the reactive near-field of an antenna such as for the distances and frequencies considered in this work. The reason is that the IPD (reference levels) does not appropriately correlate with the APD (basic restrictions) in the reactive near-field [17]. Therefore, the comparison between the APD and IPD is provided here for research purposes and the observations from this comparison are in accordance with the ICNIRP guideline.

If the two IPD expressions are compared, it can be seen that on average $S_{\mathrm{inc,2}}$ is 1.4 dB larger than $S_{\mathrm{inc,1}}$ at both 6 and 10 GHz. For the studied distances to the antenna, a decrease in the difference between these expressions when moving away from the antenna is observed.

2) FCC requirements: The second group includes $SAR_{1\mathrm{g}}$ and $S_{\mathrm{inc,2}}$ with regard to the respective FCC limit values; the FCC requires IPD assessment using $S_{\mathrm{inc,2}}$ [34]. The FCC $SAR_{1\mathrm{g}}$ limit only applies up to 7 GHz at present, but we hypothetically use the same limit value at 10 GHz in this study. The exposure ratio results of the second group are presented in Tables III and IV at 6 and 10 GHz, respectively.

TABLE III: Peak exposure ratios (ER) for SAR_{1g} and $S_{inc,2}$, when the FCC requirements are considered, at 6 GHz for different distances d obtained by simulations.

Antenna	d (mm)	Exposure ratio	
		ER_{SAR1g}	$ER_{S_{inc,2}}$
Dipole	4	0.94	0.53
	5	0.70	0.45
	6	0.51	0.39
	7	0.37	0.34
	8	0.28	0.30
	9	0.21	0.27
	10	0.17	0.24
PIFA	4	0.21	0.60
	5	0.16	0.49
	6	0.13	0.40
	7	0.11	0.34
	8	0.10	0.29
	9	0.08	0.25
	10	0.08	0.22
IFA	4	0.39	0.58
	5	0.27	0.44
	6	0.20	0.34
	7	0.15	0.28
	8	0.12	0.23
	9	0.09	0.19
	10	0.07	0.16

TABLE IV: Peak exposure ratios (ER) for SAR_{1g} and $S_{inc,2}$, when the FCC requirements are considered, at 10 GHz for different distances d obtained by simulations.

Antenna	d (mm)	Exposure ratio	
		ER_{SAR1g}	$ER_{S_{inc,2}}$
Dipole	4	0.75	0.61
	5	0.54	0.52
	6	0.39	0.45
	7	0.30	0.40
	8	0.24	0.35
	9	0.20	0.31
	10	0.17	0.28
PIFA	4	0.45	0.72
	5	0.34	0.58
	6	0.28	0.47
	7	0.24	0.40
	8	0.22	0.34
	9	0.21	0.29
	10	0.21	0.26
IFA	4	0.40	0.45
	5	0.25	0.33
	6	0.18	0.26
	7	0.13	0.20
	8	0.10	0.17
	9	0.08	0.14
	10	0.07	0.12

The data show that if considering all antennas and distances d, the exposure ratios of $S_{inc,2}$ are 2.3 and 1.5 dB larger than those of SAR_{1g} at 6 and 10 GHz on average, respectively. Exception is observed for the dipole antenna where SAR_{1g} has higher exposure ratios than $S_{inc,2}$ in 4 out of 7 cases (for d in the range 4 - 7 mm) at 6 GHz and in 2 out of 7 cases (for d = 4 and 5 mm) at 10 GHz. Nonetheless, in majority of the study cases, the exposure ratio of 1-g SAR is lower than that of $S_{inc,2}$.

IV. Estimation of APD based on SAR

A way to evaluate the peak spatial-average APD by using the peak spatial-average SAR has been introduced in [31].
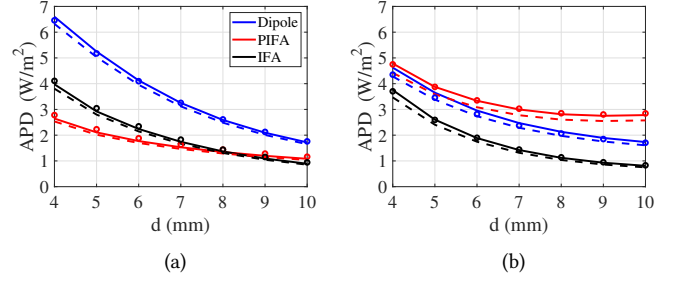

Fig. 4: Peak values of the spatial-average APD calculated by using Eq. (2) (solid line), Eq. (5.1) (dashed line), and Eq. (5.2) (circles) for different distance d antenna-phantom at: (a) 6, and (b) 10 GHz.

More precisely, two estimation formulae relating the two metrics have been proposed [31]:

$$S_{ab,1} = 20\, SAR_{8g} \tag{5.1}$$
$$S_{ab,2} = 25\, SAR_{10g} \tag{5.2}$$

where SAR_{8g} is the peak spatial-average SAR in a cube of tissue of mass 8 g, and 20 and 25 are conversion factors given in kg/m^2. The above equations are for APD averaged over a square area of 4 cm^2; in a similar way, the APD averaged over 1 cm^2 can be estimated via SAR_{1g} [31].

This method for evaluation of the peak spatial-average S_{ab} has been validated for a Hertzian dipole, half-wavelength dipole, pyramidal horn antenna with slotted array source, and cavity-fed dipole array [31]. In this paper, the same formulae were applied to the used realistic UE antennas. Fig. 4 shows the peak S_{ab} calculated by using Eq. (2), peak $S_{ab,1}$ by Eq. (5.1), and peak $S_{ab,2}$ by Eq. (5.2). The results from the two approximations $S_{ab,1}$ and $S_{ab,2}$ match well with the simulated peak S_{ab}. The absolute value of the mean difference (considering all antennas and distances d together) between peak S_{ab} and peak $S_{ab,1}$ is around 0.2 dB at 6 GHz and around 0.3 dB at 10 GHz, while between peak S_{ab} and peak $S_{ab,2}$ is around 0.2 dB (this is actually the only case where the mean S_{ab} is lower than the mean $S_{ab,2}$) at 6 GHz and 0.03 dB at 10 GHz. According to these results, the peak spatial-average SAR might be used to estimate the peak spatial-average APD for UE antennas operating at frequency between 6 and 10 GHz.

V. Experimental Verification

The dipole and PIFA antenna models were manufactured, and photographs of the prototypes are shown in Fig. 5(a) and (b), respectively. The completed mockup (the antenna was placed inside the plastic case) is shown in Fig. 5(c). A coaxial cable, the same as the one employed in the simulations, was used for feeding the antenna. The distance of 1 mm between the antenna surface and the inner wall of the mobile phone case was ensured by placing a layer of styrofoam, whose dielectric properties are close to those of air, with such thickness.
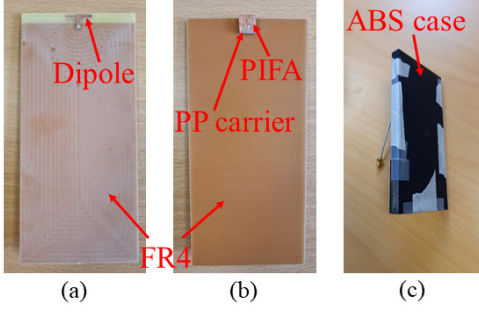
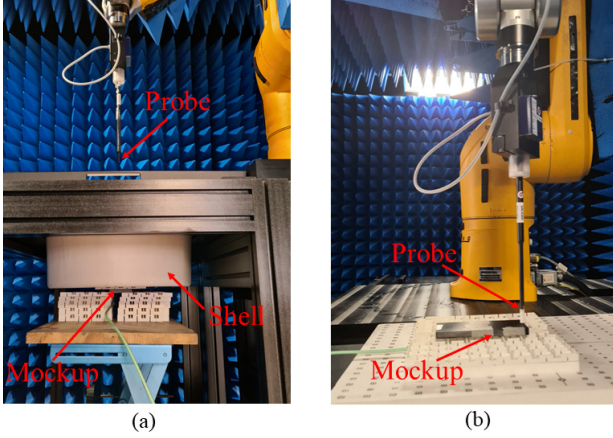Fig. 5: Photographs of the fabricated antennas: (a) dipole, and (b) PIFA. The final mockup is shown in (c).

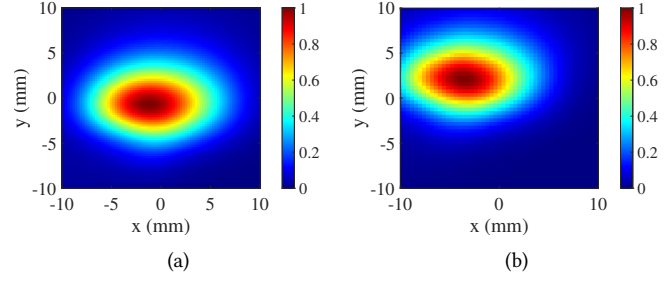Fig. 6: Test setup for measuring: (a) SAR, and (b) IPD.

Fig. 7: Normalized distribution (on the phantom top-plane) of the local SAR: (a) simulated and (b) measured at 6 GHz for dipole antenna for distance d = 4 mm.

A. SAR measurements

The SAR levels generated by the fabricated antennas were evaluated in a semi-anechoic chamber using the SAR measurements system presented in Fig. 6(a). It consisted of a DASY6 professional dosimetric system together with an isotropic E-field probe EX3DV4 and a flat phantom (Schmid & Partner Engineering AG (SPEAG), Switzerland). The shell was an elliptical open-top container with length 600 mm, width 400 mm, and thickness 2 mm; it was filled to a depth of 150 mm with the HBBL-600-6000v5 head tissue simulating liquid. The liquid with density ρ = 1000 kg/m^2 was kept at a temperature between 22.5° and 23.0° C. The DAK-3.5 Dielectric Probe Kit was used to measure the liquid dielectric properties and the medium had ϵ_r = 33.93 and σ = 5.07 S/m at 6 GHz, which were within 10% of the target values specified in [24]. The SAR evaluation was conducted through measurements of the E-field magnitude inside the phantom exposed to the EMFs produced by the antennas placed underneath (in Fig. 6(a) the mockup is indicated; the probe was lifted up from the phantom for better visualization). The measurements were performed for two distances d of 4 and 9 mm (same to the distances defined previously). The scanned volume was $30\,\text{mm} \times 30$ mm $\times 30$ mm, with a sampling step of 2 mm. The accepted power, evaluated with an Agilent N1911A power meter, a Keysight N8488A average power sensor, and a Pulsar Microwave CS20-55-435/4 1451 directional coupler, was normalized to 7 dBm, as mentioned in Section III. According to the manufacturer

of the measurement equipment, the expanded uncertainty of this type of test at 6 GHz, being the frequency of interest, is $\pm 23.3\%$ (corresponds to ± 0.91 dB) for SAR_{1g} and $\pm 23.1\%$ (corresponds to ± 0.90 dB) for SAR_{10g} [42].

Comparison between the measured and simulated peak SAR (averaged over both 1 g and 10 g; the data for SAR_{10g} is presented to get better idea about the similarity between simulation and measurement results as well as to validate the numerical results for SAR_{10g} because this metric was used for the conversion to APD in Section V) is presented in Table V. If all antennas, distances, and averaging volumes are taken together, the mean difference between the simulation and measurement data is 0.4 dB. This is a small discrepancy which is due to the difference between the simulated antennas and manufactured prototypes, and because of the measurement uncertainty (the difference between the simulation and measurement results is lower than the measurement uncertainty). Therefore, the numerical and experimental results match well.

Comparison between the simulated and measured normalized (with respect to the corresponding peak value) distribution, on the phantom top-plane, of the local SAR for dipole antenna at 6 GHz for distance antenna-phantom d = 4 mm, is presented in Fig. 7. Partly the difference in the position of the peaks between simulation and measurement is due to the uncertainty in the placement of the prototype antenna in the experiment. Good matching between the simulated and measured SAR distribution is obtained. In the rest of the cases, relatively good matching between the numerical and experimental results is observed.

TABLE V: Comparison between simulated (labeled as "Sim.") and measured ("Meas.") peak spatial-average SAR - SAR_{1g} and SAR_{10g} at 6 GHz for distance d antenna-phantom of 4 and 9 mm.

Antenna	d (mm)	SAR (W/kg)			
		SAR_{1g}		SAR_{10g}	
		Sim.	Meas.	Sim.	Meas.
Dipole	4	1.50	1.36	0.26	0.24
	9	0.34	0.30	0.09	0.08
PIFA	4	0.34	0.33	0.11	0.10
	9	0.13	0.15	0.05	0.06

The measurement data for SAR_{10g} can be used to evaluate the APD through Eq. (5.2). Table VI shows a comparison between the simulated peak APD - S_{ab}, the calculated peak - $S_{ab,2}$ (evaluated by using the simulated peak SAR_{10g}), and the calculated peak - $S_{ab,meas}$ (evaluated by using the

measured peak SAR_{10g}). As shown in Fig. 4, the peak $S_{ab,2}$ approximates well the peak S_{ab}, i.e. Eq. (5.2) gives good approximation. This together with the good matching between the simulated and measured peak spatial-average SAR leads to that $S_{ab,meas}$ gives good approximation of S_{ab} for the studied cases.

TABLE VI: Comparison between the simulated peak APD - S_{ab}, calculated peak - $S_{ab,2}$ based on the simulated peak SAR_{10g}, and calculated peak - $S_{ab,meas}$ based on the measured peak SAR_{10g} at 6 GHz for distance d antenna-phantom of 4 and 9 mm. For the calculations, Eq. (5.2) is used as SAR_{10g} is either the simulated or measured one depending on the case.

Antenna	d (mm)	APD (W/m^2)		
		S_{ab}	$S_{ab,2}$	$S_{ab,meas}$
Dipole	4	6.60	6.46	6.03
	9	2.10	2.13	1.89
PIFA	4	2.65	2.78	2.59
	9	1.20	1.28	1.41

B. IPD Measurements

The IPD values were obtained from the measurements of the $E-$field in free space using the test setup in Fig. 6(b). The antenna under test (AUT) was placed above the SPEAG mmWave free-space phantom consisting of a 40 mm thick Rohacell plate with $\tan(\delta) \leq 0.05$ and relative permittivity $\epsilon_r \leq 1.2$, which approximates free-space conditions, without distorting the field. The measurements were performed with DASY6 mmWave module and the EUmmWV3 probe along three planes parallel to the AUT and at 6 GHz and for distances d of 4, 7, and 10 mm. The size of the measured planes was $200\,\text{mm} \times 200$ mm with a sampling step of $\lambda/8$. Then the $E-$ and $H-$field for the evaluation of the IPD were reconstructed through the equivalent source reconstruction (ESR) algorithm presented in [43]. The accepted power was normalized to 7 dBm, as discussed above. The expanded uncertainty of the IPD measurement, according to the manufacturer of the test equipment, is ±1.51 dB at 6 GHz [44].

A comparison between the simulated and measured peak average IPD, defined by each of the two ways, is shown in Table VII. The same reasons for the discrepancy between the simulation and measurement results, as the ones mentioned above, are valid. If all antennas, distances, and definitions of S_{inc} are considered together, the mean difference between the numerical and experimental data is 0.8 dB, which is lower than the measurement uncertainty. Therefore, simulation and measurement results generally agree well. The difference between the experimental and numerical IPD results is higher than that in the case of SAR. The reason for that can be attributed to the higher measurement uncertainty for the IPD test compared to that for the SAR.

Fig. 8 shows comparison between the simulated and measured normalized (with respect to the corresponding peak value) distribution of the averaged over a square surface with 4 cm^2 area $S_{inc,1}$ and $S_{inc,2}$ at 6 GHz for dipole antenna for distance d = 4 mm. Part of the difference in the position of the peaks in the measurement, compared to that in the simulation, is due to the uncertainty in the placement of

TABLE VII: Comparison between simulated (labeled as "Sim.") and measured ("Meas.") peak spatially-averaged IPD $S_{inc,1}$, and $S_{inc,2}$ at 6 GHz for distances d of 4, 7, and 10 mm.

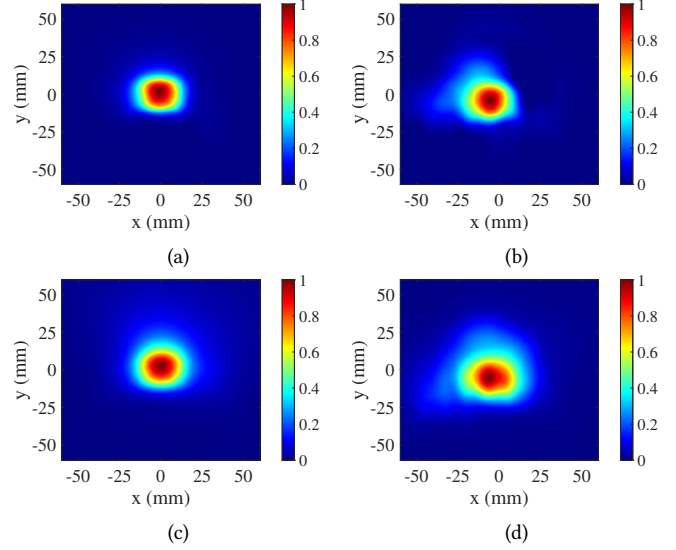| Antenna	d (mm)	S_{inc} (W/m^2)			
		$S_{inc,1}$		$S_{inc,2}$	
		Sim.	Meas.	Sim.	Meas.
Dipole	4	3.50	2.75	5.29	4.45
	7	2.63	2.10	3.44	2.63
	10	2.00	1.50	2.43	1.81
PIFA	4	4.01	3.58	6.00	7.83
	7	2.69	2.07	3.39	3.83
	10	1.93	1.90	2.23	2.38

Fig. 8: Normalized distribution of simulated and measured averaged over a square surface with 4 cm^2 area: (a) simulated $S_{inc,1}$, (b) measured $S_{inc,1}$, (c) simulated $S_{inc,2}$, and (d) measured $S_{inc,2}$ at 6 GHz for dipole antenna for distance d = 4 mm.

the prototype antenna in the experiment. The distribution of both numerical $S_{inc,1}$ and $S_{inc,2}$ is similar to that of the experimental ones. Relatively good matching between the simulated and measured IPD distributions in the other studied cases is also observed.

VI. Concluding Remarks

In this paper, a study comparing different exposure metrics for portable devices has been presented. The metrics of interest have been SAR averaged over 1 g, APD, and two expressions of IPD (considering the normal component or the magnitude of the real part of the Poynitng vector) averaged over a square surface with 4 cm^2 area. Two different frequencies - 6 and 10 GHz have been used in the investigation, and the evaluation distance for the exposure from the antennas has been varied from 4 to 10 mm, which is close (physically and electrically) to the antenna.

Both the ICNIRP guidelines and the FCC requirements for general public have been considered for quantifying the exposure ratios in this paper. The following has been observed (keeping in mind that the study is limited):

- If all studied cases are considered together, the exposure ratios of APD are on average some 1.2 dB higher than the exposure ratios of IPD (calculated by using the

magnitude of the real part of the Poynting vector), and in the range between 0.6 dB lower and 4.0 dB higher. These findings are in accordance with what prescribed by the ICNIRP guidelines, specifying that the IPD (reference levels) above 6 GHz does not correlate appropriately with APD (basic restrictions) in the reactive near-field of the antenna and that IPD cannot be used to determine compliance in that region. The results cannot be generalized to frequencies above 10 GHz since the ratio between IPD and APD limits is decreasing with the frequency while the electrical distance between the phantom and the source scales up with frequency.

- Considering the exposure ratios of SAR_{1g} and the magnitude of the real part of the Poynting vector as IPD with regard to the respective FCC limit values (the SAR_{1g} limit value is hypothetically applied at 10 GHz), it has been observed that $S_{inc,2}$ has higher exposure ratio than SAR_{1g} in the majority of the cases (17 out of 21 cases at 6 GHz and 19 out of 21 cases at 10 GHz); this has always been the case for IFA and PIFA antennas which are typical UE antennas.

- A method proposed in the literature to estimate the peak spatial-average APD from the peak spatial-average SAR has been checked with the used UE antennas. For the studied scenarios, it has been found that the peak spatial-average APD is well estimated by using the peak SAR averaged over either 8 g or 10 g tissue.

The simulation results have been verified through measurements of the SAR and IPD. Good matching between the numerical and experimental results has been observed. The findings in the paper are useful for the future EMF standardization activities related to compliance assessments of portable devices operating between 6 and 10 GHz.

Acknowledgment

References

[1] *User Equipment (UE) radio transmission and reception; Part 1: Range 1 Standalone*, TS 38.101-1: NR, 3GPP, Rev. 17.5.0, 2022.

[2] *User Equipment (UE) radio transmission and reception; Part 2: Range 2 Standalone*, TS 38.101-2: NR, 3GPP, Rev. 17.5.0, 2022.

[3] G. Wikström, P. Persson, S. Parkvall, G. Mildh, E. Dahlman, B. Balakrishnan *et al.*, "6G – connecting a cyber-physical world," White Paper, Ericsson, Feb. 2022. [Online]. Available: https://www.ericsson.com/en/reports-and-papers/white-papers/a-research-outlook-towards-6g

[4] *Study on IMT parameters for 6.425-7.025GHz, 7.025-7.125GHz and 10.0-10.5GHz*, RP-200513, 3GPP, 2020.

[5] K. R. Boyle, "The performance of gsm 900 antennas in the presence of people and phantoms," in *Proc. 12th Int. Conf. Antennas Propag.*, vol. 1, 2003.

[6] S. S. Zhekov and G. F. Pedersen, "Effect of dielectric properties of human hand tissue on mobile terminal antenna performance," in *Proc. 14th Eur. Conf. Antennas Propag.*, 2020.

[7] J. Krogerus, J. Toivanen, C. Icheln, and P. Vainikainen, "Effect of the human body on total radiated power and the 3-d radiation pattern of mobile handsets," *IEEE Trans. Instrum. Meas*, vol. 56, no. 6, pp. 2375–2385, 2007.

[8] C.-H. Li, E. Ofli, N. Chavannes, and N. Kuster, "Effects of hand phantom on mobile phone antenna performance," *IEEE Trans. Antennas Propag.*, vol. 57, no. 9, pp. 2763–2770, 2009.

[9] J. Ilvonen, O. Kivekas, J. Holopainen, R. Valkonen, K. Rasilainen, and P. Vainikainen, "Mobile terminal antenna performance with the user's hand: Effect of antenna dimensioning and location," *IEEE Antennas Wireless Propag. Lett.*, vol. 10, pp. 772–775, 2011.

[10] S. S. Zhekov, A. Tatomirescu, O. Franek, and G. F. Pedersen, "Study of the interaction user head-ultrawideband MIMO antenna array for mobile terminals," in *Proc. Int. Conf. Electromagn. Adv. Appl.*, 2016.

[11] B. Xu, Z. Ying, L. Scialacqua, A. Scannavini, L. J. Foged, T. Bolin, K. Zhao, S. He, and M. Gustafsson, "Radiation performance analysis of 28 GHz antennas integrated in 5G mobile terminal housing," *IEEE Access*, vol. 6, pp. 48 088–48 101, 2018.

[12] S. S. Zhekov, J. H. Mikkelsen, and G. F. Pedersen, "Over-the-air evaluation of user body loss for popular in-ear bluetooth earbuds," *Int. J. Antennas Propag.*, 2021.

[13] G. F. Pedersen, K. Olesen, and S. L. Larsen, "Bodyloss for handheld phones," in *Proc. 49th IEEE Veh. Technol. Conf.*, vol. 2, 1999.

[14] S. S. Zhekov and G. F. Pedersen, "Over-the-air evaluation of the antenna performance of popular mobile phones," *IEEE Access*, vol. 7, pp. 123 195–123 201, 2019.

[15] V. Plicanic, B. K. Lau, A. Derneryd, and Z. Ying, "Actual diversity performance of a multiband diversity antenna with hand and head effects," *IEEE Trans. Antennas Propag.*, vol. 57, no. 5, pp. 1547–1556, 2009.

[16] S. S. Zhekov, A. Tatomirescu, E. Foroozanfard, and G. F. Pedersen, "Experimental investigation on the effect of user's hand proximity on a compact ultrawideband mimo antenna array," *IET Microw. Antennas Propag.*, vol. 10, no. 13, pp. 1402–1410, Oct. 2016.

[17] ICNIRP, "Guidelines for limiting exposure to electromagnetic fields (100 kHz to 300 GHz)," *Health Phys.*, vol. 118, no. 5, pp. 483–524, May 2020.

[18] *IEEE Standard for Safety Levels with Respect to Human Exposure to Electric, Magnetic, and Electromagnetic Fields, 0 Hz to 300 GHz*, IEEE Standard C95.1-2019, 2019.

[19] *Radio Frequency Radiation Exposure Limits, Code of Federal Regulation Title 47, Part 1.1310*, FCC, 2017.

[20] K. Zhao, Z. Ying, and S. He, "EMF exposure study concerning mmWave phased array in mobile devices for 5G communication," *IEEE Antennas Wireless Propag. Lett.*, vol. 15, pp. 1132–1135, 2016.

[21] B. Thors, D. Colombi, Z. Ying, T. Bolin, and C. Törnevik, "Exposure to RF EMF from array antennas in 5G mobile communication equipment," *IEEE Access*, vol. 4, pp. 7469–7478, 2016.

[22] B. Xu, K. Zhao, Z. Ying, D. Sjöberg, W. He, and S. He, "Analysis of impacts of expected RF EMF exposure restrictions on peak EIRP of 5G user equipment at 28 GHz and 39 GHz bands," *IEEE Access*, vol. 7, pp. 20 996–21 005, 2019.

[23] W. He, B. Xu, Y. Yao, D. Colombi, Z. Ying, and S. He, "Implications of incident power density limits on power and EIRP levels of 5G millimeter-wave user equipment," *IEEE Access*, vol. 8, pp. 148 214–148 225, 2020.

[24] *Measurement procedure for the assessment of specific absorption rate of human exposure to radio frequency fields from hand-held and body-mounted wireless communication devices – Part 1528: Human models, instrumentation, and procedures (Frequency range of 4 MHz to 10 GHz)*, Standard IEC/IEEE 62209-1528, 2020.

[25] B. Xu, M. Gustafsson, S. Shi, K. Zhao, Z. Ying, and S. He, "Radio frequency exposure compliance of multiple antennas for cellular equipment based on semidefinite relaxation," *IEEE Trans. Electromagn. Compat.*, vol. 61, pp. 327–336, 2019.

[26] S. S. Zhekov, K. Zhao, O. Franek, and S. Zhang, "Test reduction for power density emitted by handset mmwave antenna arrays," *IEEE Access*, vol. 9, pp. 23 127–23 138, 2021.

[27] J. Lundgren, J. Helander, M. Gustafsson, D. Sjöberg, B. Xu, and D. Colombi, "A near-field measurement and calibration technique: Radio-frequency electromagnetic field exposure assessment of millimeter-wave 5G devices," *IEEE Antennas Propag. Mag.*, vol. 63, pp. 77–88, 2021.

[28] W. He *et al.*, "Fast power density assessment of 5G mobile handset using equivalent currents method," *IEEE Trans. Antennas Propag.*, vol. 69, pp. 6857–6869, 2021.

[29] S. S. Zhekov, M. Yao, O. Franek, K. Zhao, and S. Zhang, "Emf exposure of human head by handset mmwave phased antenna array," in *Proc. 16th Eur. Conf. Antennas Propag.*, 2022, pp. 1–5.

[30] M. S. Morelli, S. Gallucci, B. Siervo, and V. Hartwig, "Numerical analysis of electromagnetic field exposure from 5G mobile communications at 28 GHz in adults and children users for real-world exposure scenarios," *Int. J. Environ. Res. Public Health*, vol. 18, no. 3, 2021.

[31] T. Samaras, A. Christ, and N. Kuster, "Compliance assessment of the epithelial or absorbed power density below 10 GHz using SAR measurement systems," *Bioelectromagnetics*, vol. 42, no. 6, pp. 484–490, 2021.

[32] *Conversion method of specific absorption rate to absorbed power density for the assessment of human exposure to radio frequency electromagnetic fields from wireless devices in close proximity to the head and body - Frequency range of 6 GHz to 10 GHz*, IEC PAS 63446:2022, 2022.

[33] (2019, Apr.) RF exposure procedures. Laboratory Division, Office of Engineering and Technology, FCC. [Online]. Available: https://transition.fcc.gov/oet/ea/presentations/files/apr19/4.0-RF-Exposure-Panel-FINAL.pdf

[34] *Selected Mobile and Portable Device RF Exposure Policies and Procedures*, FCC TCB Workshop presentations, 2021.

[35] K. Zhao, S. Zhang, Z. Ying, T. Bolin, and S. He, "SAR study of different mimo antenna designs for lte application in smart mobile handsets," *IEEE Trans. Antennas Propag.*, vol. 61, no. 6, pp. 3270–3279, 2013.

[36] M. Jensen and Y. Rahmat-Samii, "The electromagnetic interaction between biological tissue and antennas on a transceiver handset," in *Proc. IEEE Antennas Propag. Soc. Int. Symp. URSI Nat. Radio Sci. Meet.*, vol. 1, 1994, pp. 367–370 vol.1.

[37] S. S. Zhekov, O. Franek, and G. F. Pedersen, "Dielectric properties of human hand tissue for handheld devices testing," *IEEE Access*, vol. 7, pp. 61 949–61 959, 2019.

[38] C. Di Paola, I. Syrytsin, S. Zhang, and G. F. Pedersen, "Investigation of user effects on mobile phased antenna array from 5 to 6 GHz," in *12th Eur. Conf. Antennas Propag.*, 2018, pp. 1–5.

[39] S. S. Zhekov, O. Franek, and G. F. Pedersen, "Dielectric properties of common building materials for ultrawideband propagation studies [measurements corner]," *IEEE Antennas Propag. Mag.*, vol. 62, no. 1, pp. 72–81, 2020.

[40] *IEEE Guide for the Definition of Incident Power Density to Correlate Surface Temperature Elevation*, IEEE Standard 2889-2021, 2021.

[41] *Product standard to demonstrate the compliance of wireless communication devices with the basic restrictions and exposure limit values related to human exposure to electromagnetic fields in the frequency range from 30 MHz to 6 GHz: hand-held and body mounted devices in close proximity to the human body*, Standard EN 50566:2017, 2017.

[42] *DASY6 Module SAR System Handbook*, Schmid & Partner Engineering AG (Speag).

[43] K. S. Cujia, A. Fallahi, S. Reboux, and N. Kuster, "Experimental exposure evaluation from the very close near-to the far-field using a multiple-multipole source reconstruction algorithm," *IEEE Trans. Antennas Propag.*, 2022.

[44] *DASY6 Module mmWave System Handbook*, Schmid & Partner Engineering AG (Speag).